Front. Earth Sci. 2022, 16(2): 446–464
https://doi.org/10.1007/s11707-021-0874-0

RESEARCH ARTICLE

Variations in the effective and bankfull discharge for suspended sediment transport due to dam construction

Fan CHEN[1,2], Li CHEN (✉)[1], Wei ZHANG[1], Jing YUAN[3], Kanghe ZHANG[1]

1 State Key Laboratory of Water Resources and Hydropower Engineering Science, Wuhan University, Wuhan 430072, China
2 Changjiang Institute of Survey, Planning, Design and Research, Wuhan 430010, China
3 Bureau of Hydrology, Changjiang Water Resources Commission, Wuhan 430010, China

Abstract A varied class method is applied to calculate the effective discharges and their variations after the Three Gorges Dam (TGD) construction based on the mean daily flow discharge and suspended sediment concentration field data from 1981 to 2016. For comparison, the bankfull discharges are also determined according to the cross-section profiles and flow discharge-stage relations. Our results show that a bimodal effective discharge curve usually exists at the fixed sites, which generates two effective discharges (Q_{e1} and Q_{e2}) within the moderate flow range. Under the quasi-equilibrium circumstances of the pre-dam period, effective discharges are closely related to the mean annual runoff, with a narrow range of regional variations in occurrence frequency. Our analyses draw the conclusion that the relatively higher unsaturation degrees of the pre-dam effective discharges caused by dam interception and riverbed coarsening are the primary cause of the increase in effective discharges from Yichang to Shashi, while the more frequent low and medium discharges due to flow regulation drive the decrease in effective discharges from Jianli to Datong. The slightly elevated flood levels and descending bankfull levels collaboratively result in the decrease of bankfull discharges from Yichang to Shashi, while the lowered bed elevation causes the increase in bankfull discharges from Luoshan to Datong. Overall, the bankfull discharge in the Middle and Lower Yangtze River is larger than effective discharge and approaches the 1.5- year recurrence interval discharge.

Keywords effective discharge, bankfull discharge, unsaturation degree, flow-sediment regimes, Middle and Lower Yangtze River, Three Gorges Dam

Received January 11, 2020; accepted January 5, 2021

E-mail: chenliwuhee@whu.edu.cn

1 Introduction

Finding one representative flow class has been appealing in channel maintenance, channelization design, ecological management and river restoration since last century (Ashmore and Day, 1988; Andrews and Nankervis, 1995; Biedenharn et al., 2000; Shields et al., 2003; Doyle et al., 2005; Schmidt and Morche, 2006; Bunte et al., 2014). The pioneering work done by Wolman and Miller (Woloman and Miller, 1960) made it possible for the first time to quantitatively evaluate the geomorphic work by different flow events, and after that, magnitude-frequency analysis method proposed by them was frequently used to decide the flow discharge that transported the largest amount of sediment over the long term (Andrews, 1979; Ashmore and Day, 1988; Nash, 1994; Sichingabula, 1999; Emmett and Wolman, 2001; Mckee, 2002; Lenzi et al., 2004; Gomez et al., 2007; Ma et al., 2010; Bunte et al., 2014). That flow was referred as the effective discharge and advised to have a recurrence interval of one to two years (Woloman and Miller, 1960; Leopold et al., 1964; Emmett and Wolman, 2001; Lenzi et al., 2006).

An analytical solution of effective discharge was derived by Nash on the premise of a lognormal distribution of flow frequency and a power function of sediment rating curve (Nash, 1994). However, the predicted recurrence interval of effective discharge from the devised unimodal effective discharge curve was in poor agreement with that observed in 55 USA streams. Due to seasonal and hysteresis effects, considerable differences existed in the rating curves during warm or cold season, and on the rising or falling stage (Walling, 1977; Gunsolus and Binns, 2018). On the other hand, both human activities (Chen et al., 2019) and sharp changes of natural conditions (Ashraf et al., 2016; Rickenmann et al., 2016) strongly impacted the flow frequency, making it deviate far from the lognormal

distribution. Therefore, a multi-modal effective discharge curve was often observed, and owing to the differences in stream size, physiography, regional environment and anthropogenic intervention, the calculated effective discharge curves displayed diverse forms. For example, Ashmore and Day (1988) investigated the effective discharges for suspended sediment load at 21 sites in the Saskatchewan River Basin and summarized five kinds of effective discharge histograms, which had one or more peaks of similar or quite different magnitudes. Sichingabula (1999) later found various sediment-discharge regimes observed in the Fraser River Basin could also be classified into four categories as described by Ashmore. After inquiring the field data at 10 hydrometric stations in the Wuding River Basin, Ma et al. (2010) differentiated the effective discharge histograms into four types generally having multi-peak forms within the moderate flow range. Also, big differences exhibited in the recurrence interval and flow duration of effective discharges. In many cases, the observed recurrence interval of effective discharge could be much less frequent than the suggested 1–2 years and be widely variable (Nash, 1994; Lenzi et al., 2006), even ranging between 1 and 32 years (Willams, 1978).

Besides the objective differences in effective discharge for different streams, the variations in field data series length and computation methods of effective discharge could also contribute to diverse outcomes. In definition of the computation terms, Andrews (1979) suggested a minimum of 5-year record and Biedenharn et al. (2000) argued only a record ranging 10–20 years was sufficient to fully represent the morphological significances of all flows. Among all the influencing factors, the number or size of flow class interval was considered to be the cause of the largest uncertainty in effective discharge computation (Yevjevich, 1972; Crowder and Knapp, 2005; Ma et al., 2010). According to the earlier studies, the choice of class interval was purely based on empirical judgment and preferred a fixed value (Sichingabula, 1999) until Crowder and Knapp (2005) firstly presented an iterative approach to determine the class interval. But the criteria for stopping iteration such as possessing at least one flow event within each interval could not be always met, hence, the application of this method in streams with large and abrupt flow discharge variations was limited. Another varied class method based on the standard deviation S of the full flow record was proposed by Ma et al. (2010), who compared the impacts on effective discharge computation of different intervals and finally determined the interval to be 0.5S. This method was also successfully applied to the effective discharge computation of a dammed river (Li et al., 2018b).

In the long run of finding the characteristic discharges that produce steady channel dimensions, effective discharge was usually discussed together with bankfull discharge, which was referred as the flow discharge exactly filling the channel to the floodplains (Willams, 1978). Since the bankfull discharge depicted the boundary of the whole active channel, it was thought to have the largest morphological significance in forming channels (Dunne and Leopold, 1978; Willams, 1978). Almost an equal number of articles confirmed and denied the equivalence between effective discharge and bankfull discharge, respectively, cautioning the replacement of effective discharge by bankfull discharge (Andrews, 1979; Ashmore and Day, 1988; Nash, 1994; Andrews and Nankervis, 1995; Sichingabula, 1999; Eaton and Lapointe, 2001; Emmett and Wolman, 2001; Vogel et al., 2003; Schmidt and Morche, 2006). Therefore, although both of the effective discharge and bankfull discharge are likely to be the key of shaping channels, the leading factors controlling their development may have a great difference.

Upstream damming is usually regarded as having the greatest anthropogenic impacts on natural rivers (Zahar et al., 2008; Pal, 2016). The modified flow processes and sediment supply regimes caused by damming changed the original balance between sediment load and flows' transport ability, and thus driving the modifications of channel morphology to match the new flow-sediment regimes (Graf, 2006; Zahar et al., 2008; Roy and Sinha, 2014). Although the hydrological and morphological changes in dammed rivers have been addressed repeatedly (Zhang et al., 2016; Chen et al., 2019), the impacts on effective and bankfull discharge variations due to dam construction have seldom been discussed. With an extreme unsaturation state of sediment-laden flows and the development of bed scouring after dam construction, channel dimensions and the relative effectiveness of different flow classes altered, which inevitably caused the changes in effective and bankfull discharges. Thus, studying the variations in effective and bankfull discharges after dam construction and revealing the reasons are of great importance to illustrate the mechanisms of riverbed evolution in the downstream reaches.

Therefore, this paper compares and analyses the effective and bankfull discharge variations in the Middle and Lower Yangtze River in China (Fig. 1). Since the complement of the Three Gorges Dam (TGD), great changes occurred in the downstream hydrodynamics and landscape processes. The aims of this paper are (i) to provide an estimate of effective and bankfull discharges at various sites in the Middle and Lower Yangtze River; (ii) to analyze the variations in effective and bankfull discharges after the TGD construction; (iii) to appraise the equivalence of effective discharge and bankfull discharge in the Middle and Yangtze River.

2 Study area

The Yangtze River, with a basin area of 1.8×10^6 km^2 flows about 6397 km. According to different regional environments and hydrogeology conditions, it can be usually

divided into the upper, middle and lower reaches (Fig. 1). The study reach in this paper is from Yichang to Datong, stretching about 1183 km. Portions of water volume and sediment load are diverted from the main stream to Dongting Lake by three outlets and then rejoin the main stream at Chenglingji. At Hankou and Hukou, flows enter the Yangtze River from Hanjiang and Poyang Lake, respectively. The sub-segment from Yichang to Dabujie is basically composed of gravel, while from Dabujie to Datong, sand is the dominant materials of riverbed. Since suspended sediment is more than 98% of the total sediment load downstream of Yichang and the bedload field data are commonly scarce (Yang et al., 2007), only the effective discharge for suspended sediment are investigated in the following analysis.

As the largest hydroelectric power plant in the world, TGD lies in the outlet of the Upper Yangtze River. Along the study reach situate the Yichang, Shashi, Jianli, Luoshan, Hankou and Datong hydrometric stations longitudinally, which are responsible for regular hydrographic measurements. After the completion of TGD, striking temporal and spatial variations occurred in the downstream channel adjustments, leading to the variability of effective and bankfull discharges.

3 Data and methods

3.1 Data collection

A great deal of cross-section profile surveys and regular hydrographic measurements have been conducted since 1960s by the Changjiang Water Resources Commssion (CWRC). The related hydrological data including the daily average flow discharge, water stage and suspended sediment concentration during 1981–2016 at the 6 hydrometric stations were collected (Fig. 2; the record length used for magnitude-frequency analysis was more than that suggested by Sichingabula (1999)).

Cross-sections near each hydrometric station were chosen to be the representative cross-sections for bankfull level identification and the post-flood cross-section profiles at the fixed sites surveyed in a specified year before 2003 and annually after 2003 were also collected. All these original data have undergone rigorous verification and uncertainty analysis following the government protocols (Dai and Liu, 2013). The surveying agencies were responsible for the quality control of field data.

3.2 Probability analysis for estimation of extreme values

The annual maximum values of daily flow discharge and suspended sediment transport rate over 35 years were used for recurrence interval (*RI*) estimation. The observed *RI* can be calculated by Weibull's plotting position formula (Singh et al., 2012):

$$RI = \frac{N+1}{R}, \tag{1}$$

where N is the total number of years and R is the rank of the observed annual maximum values in descending order. Then, appropriate fitting curves were chosen to fit the observed data and a smaller coefficient of Kolmorov-Smirnov indicates a greater goodness of fitting.

3.3 Determination of bankfull discharge

Determination of bankfull discharge is based on the

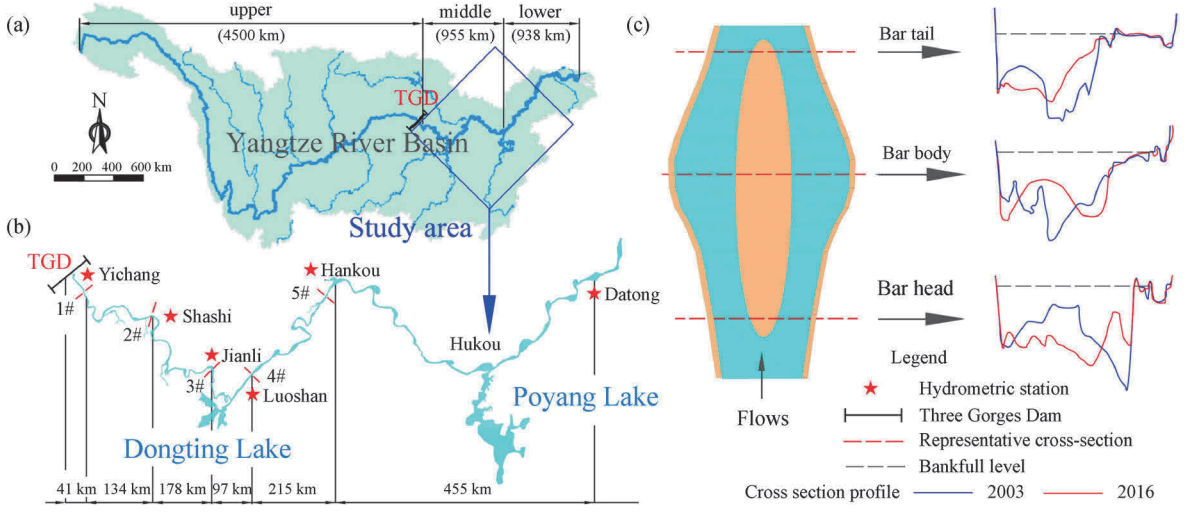

Fig. 1 Sketch image of (a) the Yangtze River Basin; (b) the study area from Yichang to Datong; and (c) the schematic plot of determining the bankfull level at the fixed sites.

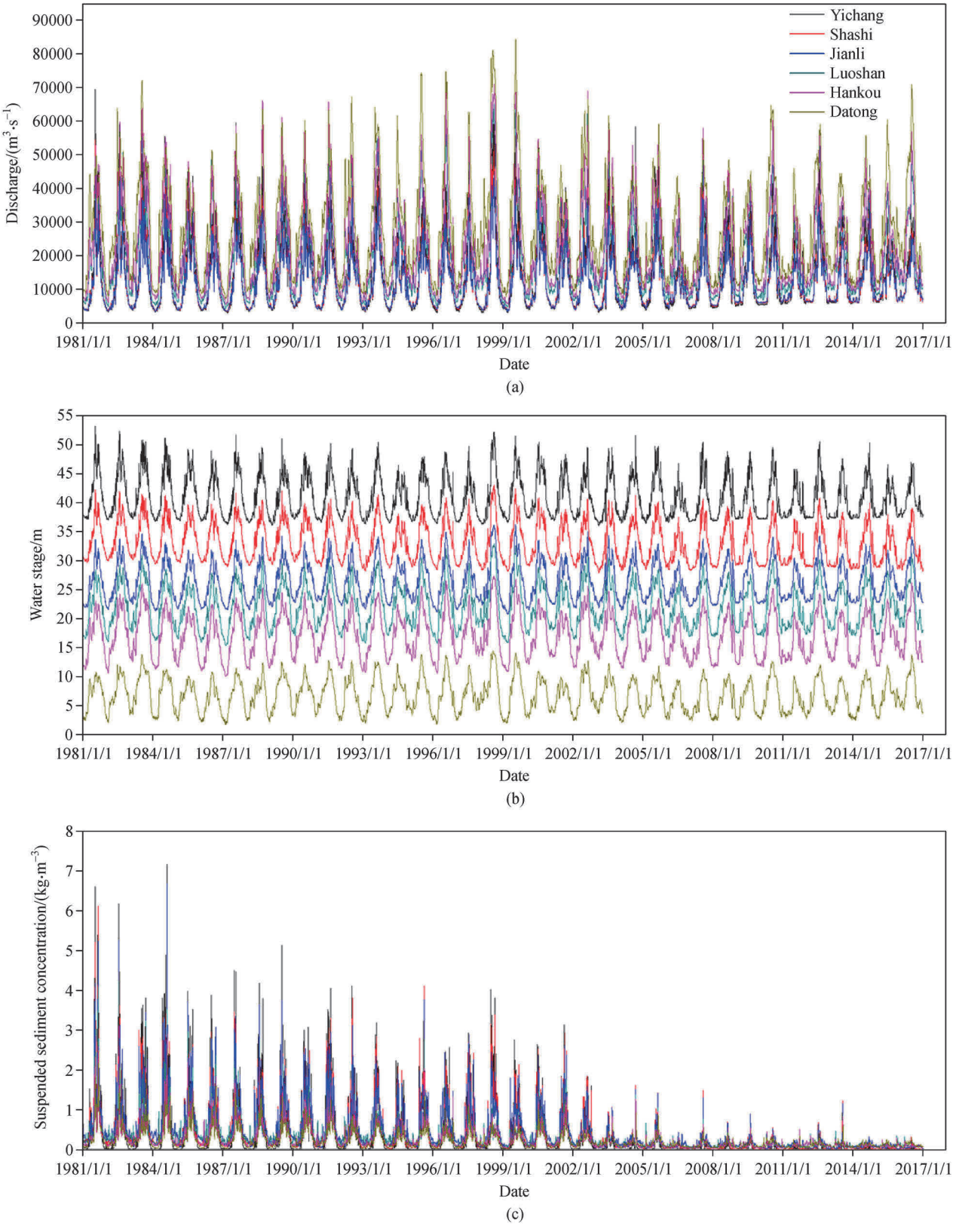

Fig. 2 Field data of the daily average (a) flow discharge; (b) water stage; and (c) suspended sediment concentration during 1981–2016.

identification of bankfull level, which in general equals to the level of the lip top of an active floodplain. At each hydrometric station, three roughly equidistant cross-section profiles respectively stretching across the head, body and tail of the mid-channel bars were inspected by eyes to obtain the bankfull levels (Fig. 1), and then the reach-averaged bankfull levels were calculated as the corresponding mathematic averages. In order to calculate the bankfull discharge, the daily average discharge versus stage data measured in the same year as the corss-section profile were fitted by power functions. The bankfull discharge at a given cross-section could be determined to be the flow discharge corresponding to the corresponding bankfull level.

The above-mentioned method can be well used to calculate the post-dam bankfull discharges owing to the sufficiency of required cross-section surveys, which were conducted annually since 2003. On the contrary, few cross-section surveys have been conducted before the TGD construction and the pre-dam bankfull levels for each year can be hardly obtained by this method. Here, we assumed that the pre-dam morphological adjustments on the floodplain were relatively small, thus the pre-dam bankfull level could be regarded as invariant and equal to the value of the particular pre-dam year. Then, the average pre-dam bankfull discharges were determined according to the average discharge versus stage curves from 1981 to 2002.

3.4 Effective discharge computation

The traditional methods of effective discharge computation often involve two fundamental assumptions: the log-normal distribution of flow frequency and power law rating curve of flow-sediment discharge (Nash, 1994; Crowder and Knapp, 2005). However, in the reaches downstream of the TGD, the distribution of flow frequency deviates from the common probability distribution functions (Fig. 3), which means these traditional approaches cannot be used directly in the present work. To avoid empirical choices of flow discharge interval and better analyze its influences on effective discharge computation, a modified approach framed in terms of equal arithmetic intervals of the standard deviation S for the analyzed discharge series (Ma et al., 2010) was adopted in the pre-dam and post- dam magnitude-frequency analysis. For each hydrometric station, the pre-dam and post-dam flow discharge records were divided into classes by five flow discharge intervals of S, 0.75S, 0.5S, 0.25S and 0.125S, respectively. Then, the total suspended sediment load transported by each flow class was calculated by summing the parts falling into each interval and plotted against the midpoint of each flow class. Finally, the effective discharges were determined to be the flow discharges corresponding to the sediment load peaks.

4 Results

4.1 Flow-sediment regimes

The flow and sediment regimes of the studied reaches can be represented by the regimes measured at the hydrometric stations. Runoff and sediment load entering into the reaches from Yichang to Jianli mainly come from the mainstream and tributaries of the Upper Yangtze River (Li et al., 2009). Since only a small portion of the mainstream water and sediment are diverted out from three outlets, the runoff decreases slightly from Yichang to Jianli. After successively absorbing the inflows from Dongting Lake at Chenglingji, from Hanjiang River at Hankou and from Poyang Lake at Hukou, the runoff increases gradually from Luoshan to Datong.

Figure 4 shows the temporal variations in water volume and sediment load. The average water volume after dam construction is about 4.022×10^{11}, 3.777×10^{11}, 3.658×10^{11},

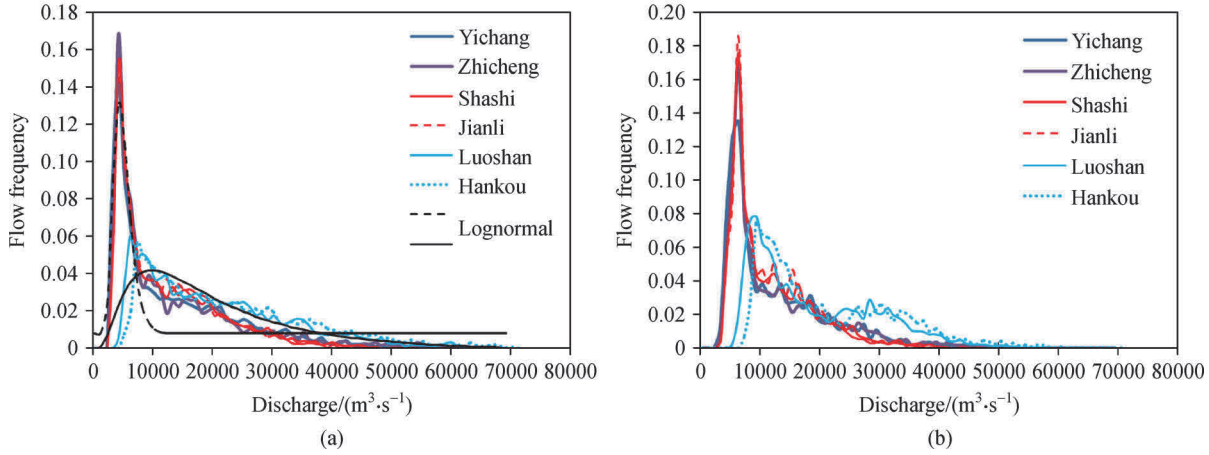

Fig. 3 Flow frequency distribution of the (a) pre-dam and (b) post-dam period.

4021×10^8, 6767×10^8 and 8582×10^8 m^3/a, respectively at Yichang, Shashi, Jianli, Luoshan and Datong, with an average decrease of 7% as compared with the values of the pre-dam period, while the sediment load decreases significantly by 50%–90%. As stated by previous studies (Zhang et al., 2016; Chen et al., 2019), although the seasonal distribution of flows is modified, the total water volume almost remains unchanged. Since large amounts of sediment are trapped in the reservoir, the sediment load suffers the most drastic reduction at Yichang, and gradually increases from Yichang to Datong (Dai et al., 2016).

After impoundment of the TGD, the low water stage exhibited an apparent decreasing trend (Qin and Chen, 2018), while the flood water stage had no decreasing trend and could be rising at certain sites (Han et al., 2017). Yet the reasons why the post-dam flood levels can get elevated or stay the same have not been fully understood and thought to be related to the increase in comprehensive channel resistance by sand coarsening (Han et al., 2017), bench vegetation (Yang et al., 2017b), climate changes (Liu et al., 2019) and human activities (Gomez et al., 2007). Figure 5 plots the stage-discharge rating curves of 1981, 2002 and 2016 at each hydrometric station. By fitting the field data with an exponential or polynomial curve, the low and flood water stage variations can be roughly estimated. It can be seen that even before the TGD construction, the diminishing sediment supply has driven the flood levels higher from Shashi to Datong over the last two decades (Wang et al., 2013). After the completion of TGD, the low and medium flow levels are lowered apparently at the close-to-dam reaches, but the flood levels tend to get further higher or stay the same from Yichang to Jianli, and slightly decline from Luoshan to Datong, whist the discharge-stage relationship at Jianli station presents a loop curve due to the fluctuation of floods and backwater effects by Dongting Lake.

However, it should be noted that the above water stage change laws could be disrupted by extreme climate conditions (Dai et al., 2008; Mei et al., 2018). Many studies reported that under the influences of an extreme drought and the TGD operation, the low water stage could be abnormally increased and the flood water stage could be obviously decreased (Chai et al., 2019a, 2019b), which highlights the importance of extreme events on water stage changes. So, it can be inferred that without the occurrence of extreme events, a more obvious water stage change trend could occur.

4.2 Recurrence intervals of peak flow and sediment discharge

In order to evaluate the occurrence frequency of floods, the empirical values of recurrence interval of annual maximum discharge are calculated. The best fitting distribution functions to empirical values and their parameters are decided by the software STATISTICA 6.1 (StatSoft, 2002), and found to be varied at different hydrometric stations (Fig. 6 and Table 1). As suggested by previous studies (Crowder and Knapp, 2005; Lenzi et al., 2006), the lognormal distributions are also found to fit reasonably (coefficients of Kolmorov-Smirnov d were all less than 0.113, which indicates a nonsignificant difference). The average differences in recurrence interval calculated by lognormal function and the most fitted function are no larger than 6% except for at Datong station, where the Weibull distribution results in extremely large recurrence intervals for less frequent flood peaks. Given the limited length of time series used in this study (35 years) and for simplicity, the lognormal distributions are recommended to calculate the recurrence intervals at all hydrometric stations in the subsequent analysis.

Similarly, recurrence intervals of annual maximum sediment transport rate are also calculated and found to fit reasonably to the lognormal distribution (Fig. 6 and Table 1), with the coefficients of Kolmorov-Smirnov *d* all less than 0.123. The recurrence intervals of annual maximum flow discharge versus sediment transport rate,

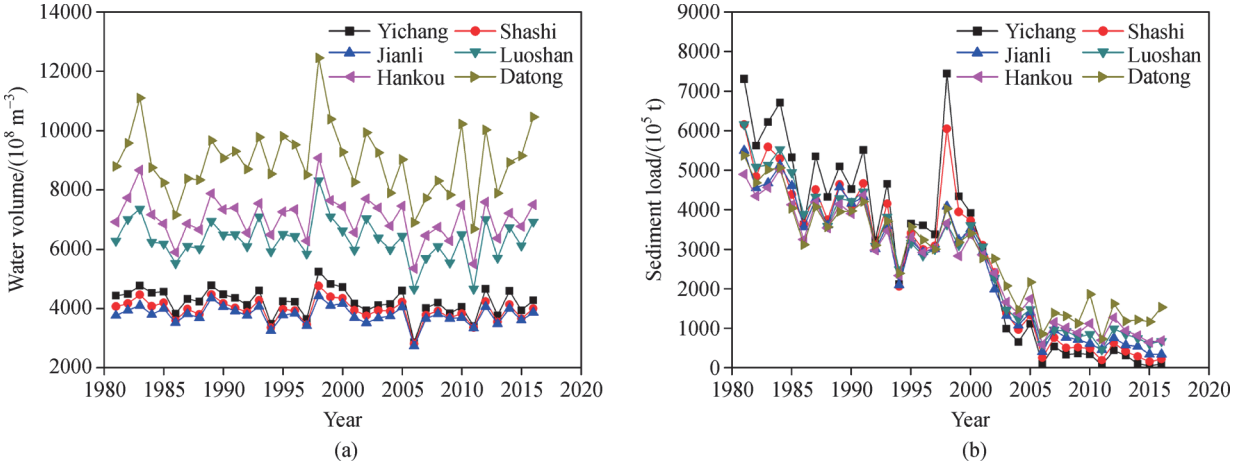

Fig. 4 Temporal variations in (a) water volume and (b) sediment load.

which to some extent reflected the incoming flow-sediment discharge relationship, are plotted in Fig. 7. During the pre-dam period, about 60% and 40% of the points are falling above and below the equality line, respectively, while during the post-dam period, these two numbers become 27% and 73%. This result reveals that the pre-dam flow-sediment regimes are characterized by a more even distribution of the low flow versus high sediment load years and high flow versus low sediment load years compared to that of the post-dam period, when channel degradation occurs due to the repeated washing by frequent unsaturated flows (Li et al., 2018a).

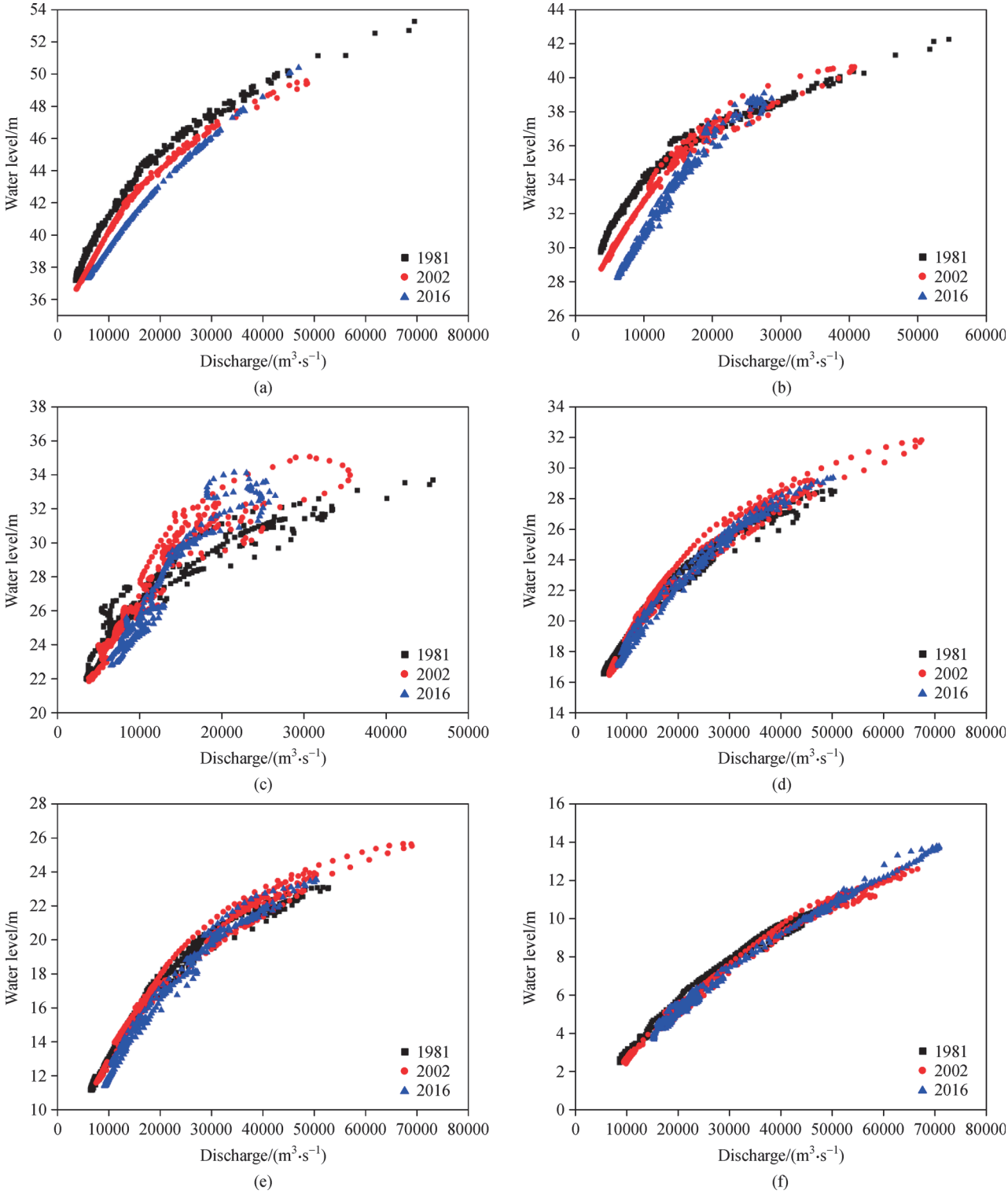

Fig. 5 Flow discharge versus water stage relationships at (a) Yichang; (b) Shashi; (c) Jianli; (d) Luoshan; (e) Hankou; (f) Datong.

Table 1 Coefficients of Kolmorov-Smirnov (d) for different fitting functions

Hydrometric station	Annual maximum peak discharge/($m^3 \cdot s^{-1}$)		Annual maximum sediment transport rate /($kg \cdot s^{-1}$)	
	d (best fitting)	d (lognormal fitting)	d (best fitting)	d (lognormal fitting)
Yichang	0.079 (Dagum)	0.096	0.066 (Dagum)	0.119
Shashi	0.080 (Gamma)	0.088	0.076 (Dagum)	0.123
Jianli	0.091 (Dagum)	0.106	0.075 (Dagum)	0.103
Luoshan	0.103 (Gamma)	0.104	0.077 (Dagum)	0.115
Hankou	0.075 (Dagum)	0.013	0.064 (Dagum)	0.083
Datong	0.083 (Weibull)	0.101	0.087 (Gamma)	0.100

Note: the best fitting functions are indicated in brackets.

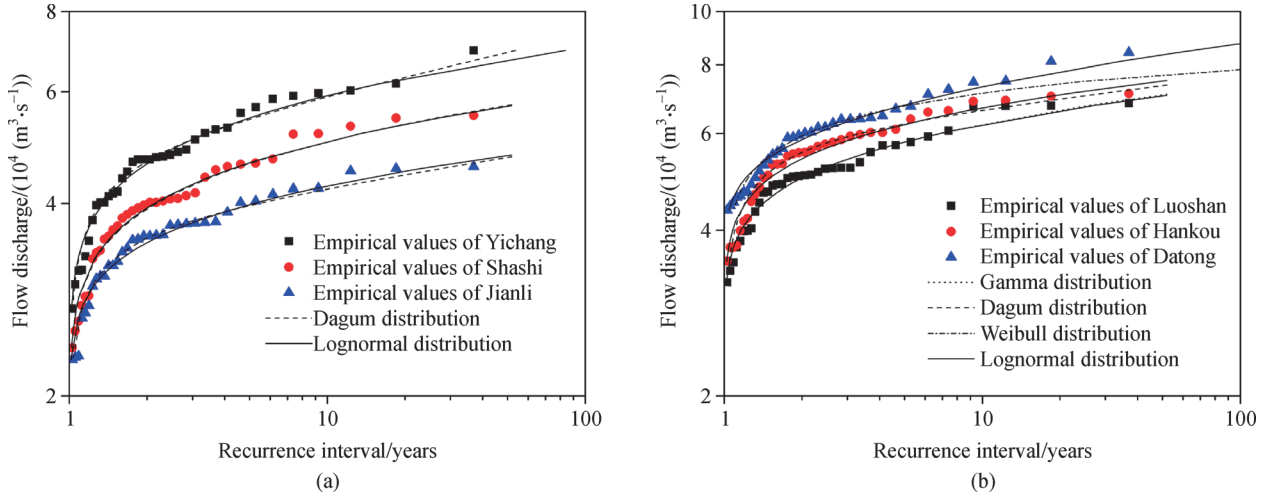

Fig. 6 Recurrence intervals of annual maximum peak discharges (a) from Yichang to Jianli and (b) from Luoshan to Datong.

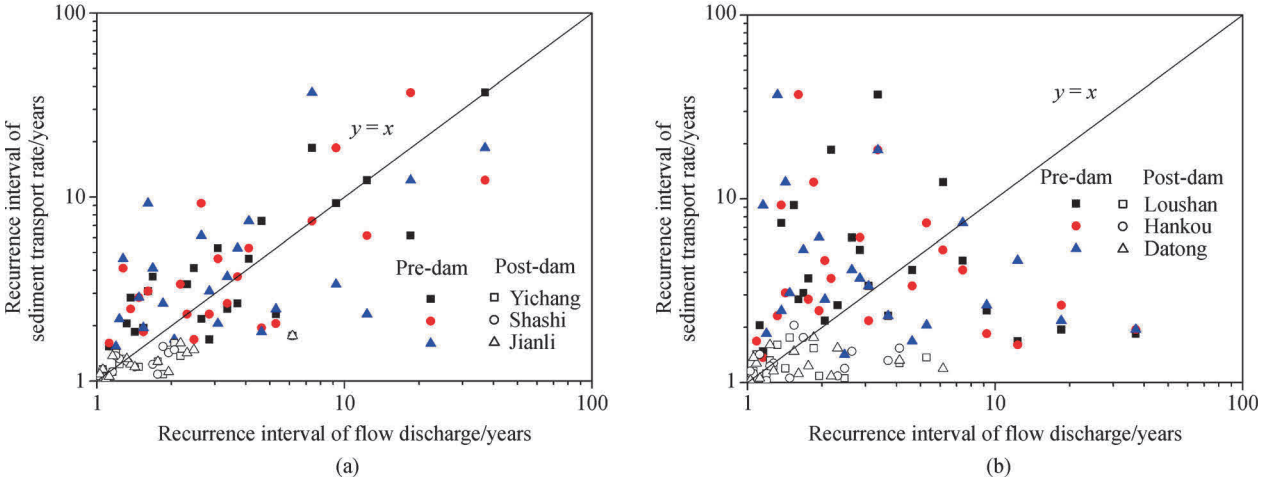

Fig. 7 Recurrence intervals of annual maximum peak discharges (a) from Yichang to Jianli; (b) from Luoshan to Datong.

4.3 Effective discharge

Figure 8 shows the calculated effective discharge curves during the pre-dam period. Generally, the effective discharge curves possess one or two peaks, the abscissas of which are all falling within the medium flow discharge ranges. With the decrease of size in flow discharge interval, the effective discharge curves are jagged, presenting more "potential" effective discharges which can transport relatively more sediment. Nevertheless, two obvious

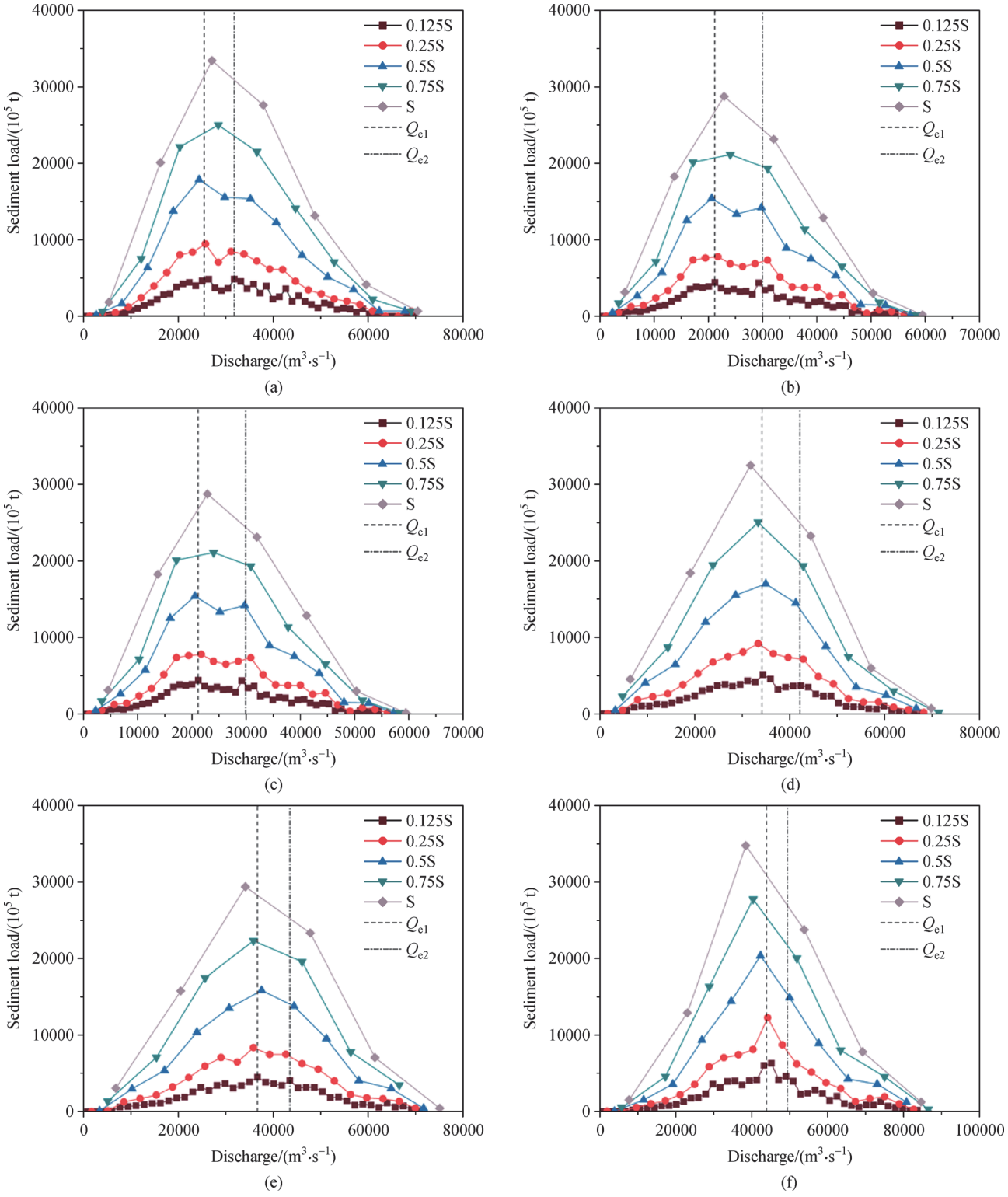

Fig. 8 Effective discharge curves at (a) Yichang; (b) Shashi; (c) Jianli; (d) Luoshan; (e) Hankou; (f) Datong.

peaks can be always identified when the interval is 0.125S–0.5S, beyond which the two peaks gradually merge and move left. Considering the abundant existence of point bars, alternative bars, central islands and other morphological units in different sizes and shapes in the Middle and Lower Yangtze River, multiple formative discharges may account for the morphological changes in terms of different channels (Surian et al., 2009). Thus, in

this sense, the flow discharges corresponding to the observed two sediment load peaks in the calculated effective discharge curves can be both called "effective discharge" (the smaller one and the larger one are denoted by Q_{e1} and Q_{e2}, respectively), transporting the largest amounts of sediment from different locations within the main channels.

In order to introduce as little deviation caused by subjective judgment as possible, two discharges are identified for each effective discharge curve calculated by 0.125S, 0.25S and 0.5S, then Q_{e1} are determined to be the averages of the corresponding three smaller ones and Q_{e2} are determined to be the averages of the corresponding three larger ones (Fig. 8). On the occasion when the 0.5S curve has only one peak such as at Luoshan, Hankou and Datong Station, Q_{e1} and Q_{e2} can be determined as the averages of the corresponding values of 0.125S and 0.25S curves. Taking this approach, the pre-dam and post-dam values (denoted by $-Q_e$ and $+Q_e$, respectively) of Q_{e1} and Q_{e2} are calculated and summarized in Table 2. Whether during the pre-dam or post-dam period, the differences between the calculated Q_{e1} and Q_{e2} range from 5000 to 10000 m^3/s according to different distances from the TGD, with an average of about 7000 m^3/s. Surprisingly, we find that a spatial diversity exists in the variability of effective discharge, with Q_{e1} at Yichang, Shashi increased by 15.1% and 12.1%, Q_{e1} at Jianli, Luoshan, Hankou, Datong reduced by 16.6%, 4.1%, 18.6% and 6.0%, respectively. Likewise, Q_{e2} at Yichang, Shashi are increased by 8.3% and 10.7%, Q_{e2} at Jianli, Luoshan, Hankou and Datong are reduced by 12.6%, 3.5%, 13.2% and 2.9%, respectively.

The flow duration curves are further plotted in Fig. 9. It can be seen that compared to the pre-dam period, the post-dam duration curves demonstrate more rugged shapes due to the seasonal distribution modification of flow discharges by reservoir operation. Duration percentages that flows equal or exceed Q_{e1} and Q_{e2} value about 13.88%–19.45% (51–71 days/a)and 5.28%–10.43% (19–38 days/a), respectively before the dam construction, while the post-dam shaping time of the above-Q_{e1} and above-Q_{e2} discharges account for about 5.28%–22% (19–80 days/a) and 1.32%–8.32% (5–31 days/a), which indicates a significant reduction in the occurrence frequency of flows that equal or exceed Q_{e2}, no matter Q_{e2} is increased or decreased in magnitude.

Generally, no big change in durations of effective

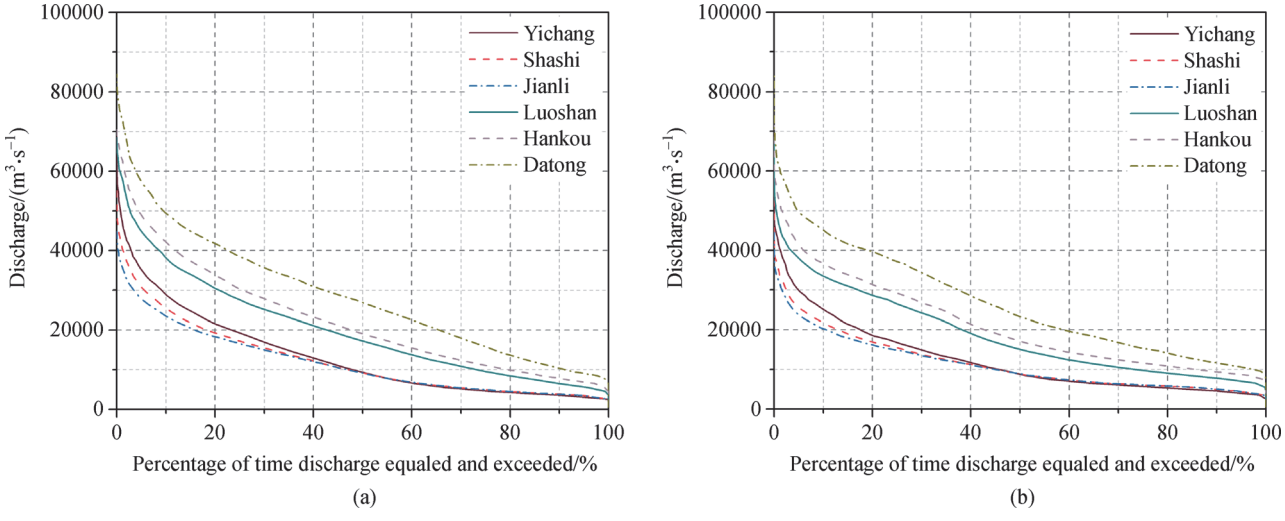

Fig. 9 Flow duration curves of the (a) pre-dam; (b) post-dam period.

Table 2 Effective, bankfull and other characteristic discharges

Hydrometric station	Q_e /($m^3 \cdot s^{-1}$)				Q_b /($m^3 \cdot s^{-1}$)		Q_c /($m^3 \cdot s^{-1}$)		Q_u	$Q_{1.5}$	$Q_{2.0}$	$-Q_e-Q_u$/($m^3 \cdot s^{-1}$)	
	$-Q_{e1}$	$+Q_{e1}$	$-Q_{e2}$	$+Q_{e2}$	$-Q_b$	$+Q_b$	$-Q_c$	$+Q_c$	/($m^3 \cdot s^{-1}$)	/($m^3 \cdot s^{-1}$)	/($m^3 \cdot s^{-1}$)	$-Q_{e1}-Q_u$	$-Q_{e2}-Q_u$
Yichang	25525	29385	31850	34495	44500	40085	45500	42500	12000	42000	46190	13525(53.0%)	19850(62.3%)
Shashi	21190	23745	29970	33185	39010	32500	40500	32800	12500	35950	39400	8690(41.0%)	17470(58.3%)
Jianli	18385	15325	26540	23210	33000	30200	33900	33200	16500	32190	34760	1885(10.3%)	10040(35.8%)
Luoshan	34120	32730	42125	40650	40000	40810	40500	41500	29500	45890	49860	4620(13.5%)	12650(30.0%)
Hankou	36695	29880	43520	37760	50500	52500	47500	53000	33500	49830	54030	3195(8.7%)	10020(23.0%)
Datong	43930	41425	49400	47945	52500	56500	54000	58800	45500	54340	58540	−1570(−3.6%)	3900(7.9%)

Note: − indicates the pre-dam variable and + indicates the post-dam variable. Q_{e1}, Q_{e2} are the effective discharges, Q_b is the bankfull discharge. Q_c is the critical discharge corresponding to the abrupt point of the flow discharge versus daily class-based sediment transport rate scatterplot (see Fig.11). Q_u means the most unsaturated flow discharge after damming (see Fig.13). $Q_{1.5}$ and $Q_{2.0}$ are the 1.5-year and 2.0-year recurrence interval discharges based on the annual flood series, respectively. The numbers in brackets mean the relative percentage changes.

discharges occurs after dam construction. Except for at Jianli station, durations of the pre-dam effective discharges at different stations are close to each other, with Q_{e1} ranging from 1.48% to 1.77% (5–7 days/a) and Q_{e2} ranging from 0.71% to 0.93% (2–4 days/a), while durations of the post-dam effective discharges vary within a broader range, with the Q_{e1} ranging from 1.08% to 2.54% (4–10 days/a) and Q_{e2} ranging from 0.35% to 1.64% (2–6 days/a). Overall, durations of the effective discharges are within the ranges reported by previous studies (Ashmore and Day, 1988; Lenzi et al., 2006) but change in a much narrower range at different sites primarily due to roughly the same geomorphological structures, climate-anthropogenic changes and hydrological-sedimentation processes of the whole Middle and Lower Yangtze River drainage area.

4.4 Bankfull discharge

The annually identified bankfull levels and discharges are plotted in Fig. 10 and the average post-dam values of them are listed in Table 2 (for lack of cross-section profiles, the values at Datong station cannot be decided here). Since the completion of TGD in 2003, the bankfull levels from Yichang to Hankou have been reduced by 0.7%–4.0%. From Fig. 10 we can also find that the post-dam bankfull discharges from Yichang to Jianli display a clear downward trend variation with an average of 40085, 32090 and 29830 m^3/s, respectively, while the bankfull discharges at Luoshan and Hankou change little with an average of 40810 and 52500 m^3/s, respectively.

Although great channel scouring occurred after the TGD construction, no such evident changes above the floodplains have been discovered (Li et al., 2018b). Since the temporal variations in bankfull levels are so subtle that the bankfull discharges can be largely decided by stage-discharge relationships, which makes the approach how the average pre-dam bankfull discharges are determined in this paper tenable (hereafter, the average bankfull discharge in terms of a period of time is denoted by Q_b). Then, by reading fitting curves of the pre-dam discharge-stage data, the pre-dam Q_b is determined and listed in Table 2. Again, a spatial diversity is found to exist in the variability of bankfull discharge. In the reaches far from the dam, the post-dam Q_b increases slightly by about 2.0% and 4.0% at Luoshan and Hankou, respectively, with an average difference of 1400 m^3/s between the pre-dam and post-dam values, while due to the slight lift of flood levels and descending bankfull levels, the post-dam Q_b at Yichang, Shashi and Jianli decreases by 9.9%, 17.7% and 9.6%, respectively, with an average difference of 4300 m^3/s between the pre-dam and post-dam values.

Before the completion of TGD, duration percentages that flows equal or exceed Q_b value about 1.58%–1.90% (5–7 days/a) from Yichang to Jianli and 4.22%–8.75% (15–32 days/a) from Luoshan to Hankou, respectively. After 2003, these duration percentages are slightly lengthened or shortened from Yichang to Jianli, but substantially reduced to 0.95%–2.82% (3–10 days/a) from Luoshan to Hankou. On the whole, the occurrence frequency of discharges equal to or larger than the post-dam Q_b varies within a narrower range, with an average of about 1.75% (6–7 days/a), despite a larger regional disparity in the magnitude of Q_b compared to the pre-dam period. Durations of the pre-dam and post-dam Q_b are almost the same, both ranging from 0.22% to 0.85% (1–3 days/a).

5 Discussion

5.1 Variations in the daily class-based sediment transport rate and associated unsaturation degree

The bankfull level is by definition delimiting the vertical boundary between the main channel and floodplains.

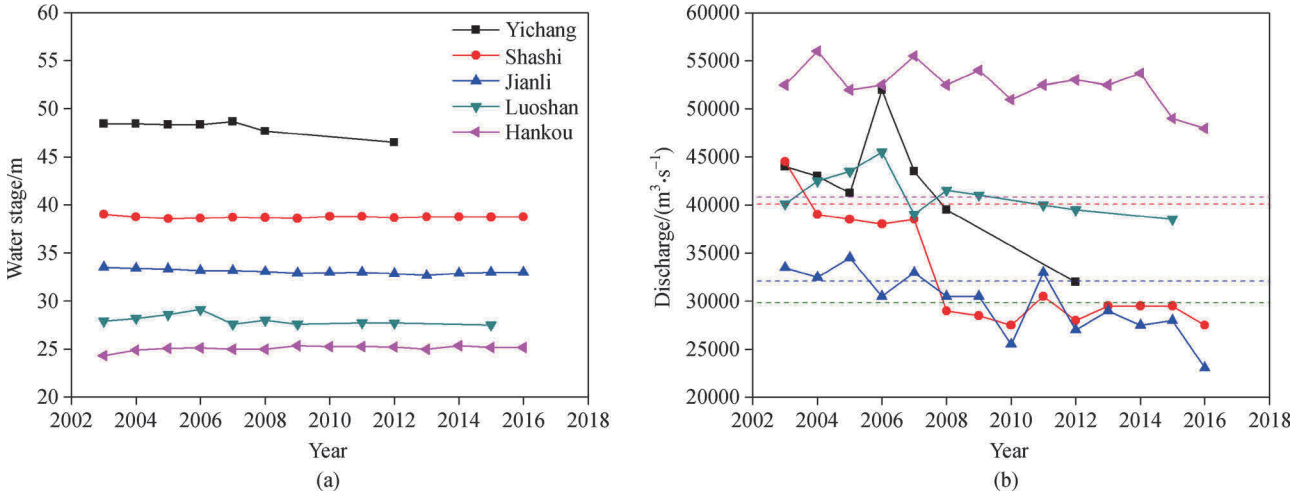

Fig. 10 Temporal variations in (a) bankfull levels; and (b) bankfull discharges after dam construction.

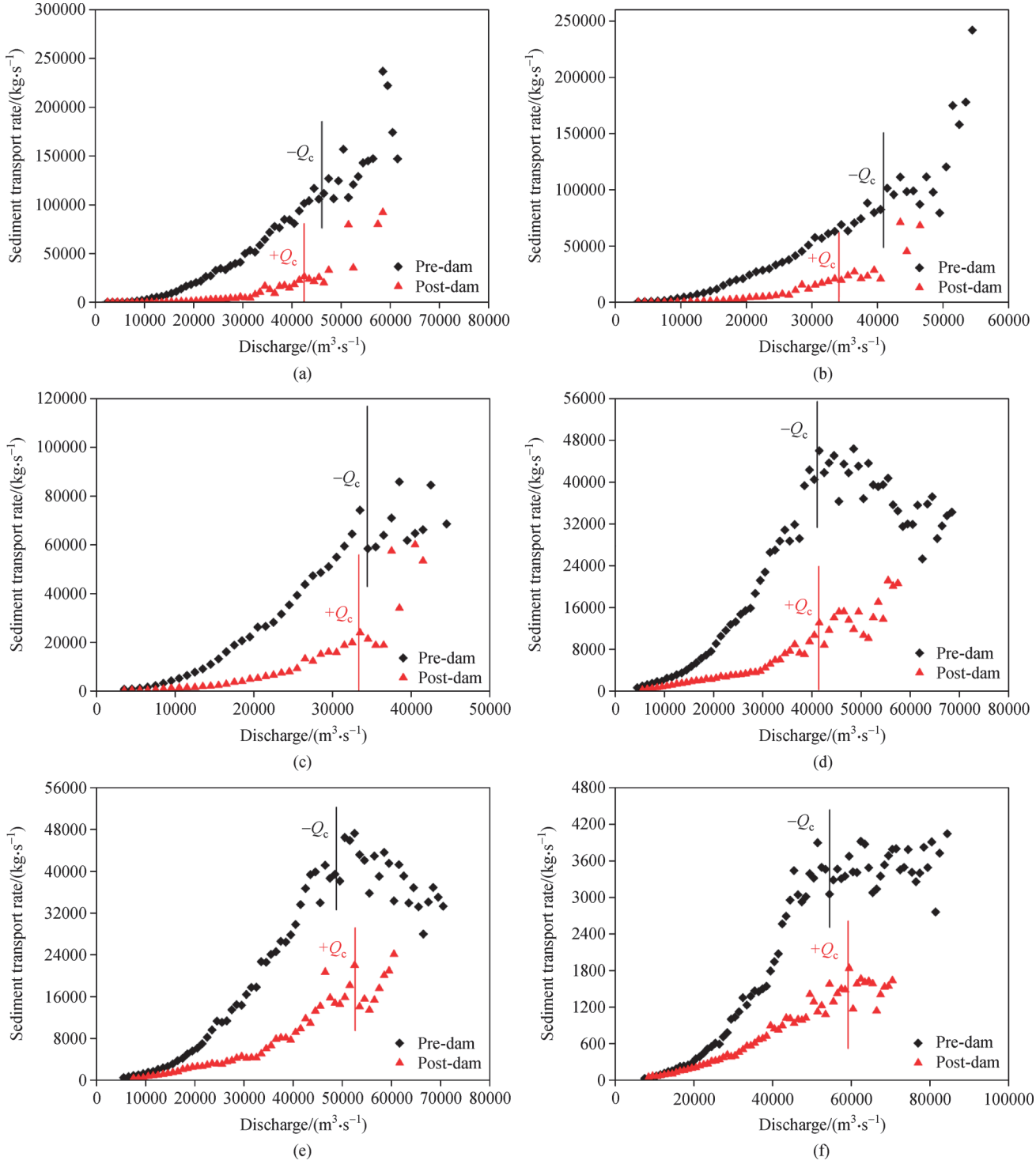

Fig. 11 Flow discharge versus daily class-based sediment transport rate relationship at (a) Yichang; (b) Shashi; (c) Jianli; (d) Luoshan; (e) Hankou; and (f) Datong.

When water stage gradually rises from a low level, flow velocity and the energy competent in sediment transport also increase, with a commonly recommended power law of sediment transport rate relationship (Walling, 1977). After water flows above the bankfull level, portions of water volume are dispersed to the floodplains and the flows suffer greater flow resistances, which hinders the increase of flow velocity and sediment transport capacity (Willams, 1978). Therefore, in theory there should be a sudden change from obviously growing to wandering around of the sediment transport rate when the ever increasing flow discharge approaches the bankfull discharge. Bearing this

in mind, we try another way to determine the bankfull discharge only based on the observed flow-sediment filed data.

Firstly, we divide the flow discharge records into classes by interval of 500 m^3/s, then the transported sediment within each flow class is summed and the number of days of discharges falling into each interval is counted. Finally, the total sediment transport rate within each flow class is divided by the counted numbers, which derives the daily class-based sediment transport rate. This method is much the same as the "mean approach" introduced by Crowder and Knapp (Crowder and Knapp, 2005) to calculate effective discharge. For the purpose here, the daily class-based sediment transport rate is plotted against the midpoint of each class in Fig. 11 and by finding the abrupt changing points, the pre-dam and post-dam critical discharges (denoted by Q_c) are determined and listed in Table 2.

Figure 12 further shows the comparison of Q_c and Q_b. As expected, the points are distributed in close proximity to the equality line, which indicates a high accuracy of determining Q_b by Q_c, and confirms the claim that bankfull discharges at the gaged sites can be obtained from the stations' rating curves (Willams, 1978). This result can be used to estimate the bankfull discharge in the case when there are more sufficient flow-sediment data instead of cross-section survey data. In the discussion below, the Q_b values at Datong are regarded as equal to the corresponding Q_c.

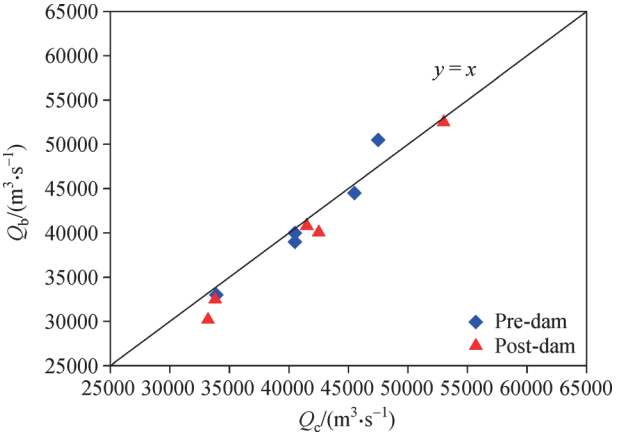

Fig. 12 Relationship between the critical discharge from Fig.11 (Q_c) and bankfull discharge (Q_b).

Similar to the variations in rating curve reported by previous studies (Zahar et al., 2008; Yuan et al., 2012; Dai and Liu, 2013), the scatterplot (Fig. 11) also demonstrates a remarkable reduction in the class-based sediment transport rate at given discharges. To weigh the decreasing degree quantitatively, the concept of flow unsaturation degree is adopted (Li et al., 2018b) and can be written as:

$$USD = (SR_{\text{pre}} - SR_{\text{post}}) \times 100/SR_{pre}, \quad (2)$$

where USD means the unsaturation degree, %; SR_{pre} and SR_{post} are the previously calculated pre-dam and post-dam daily class-based sediment transport rate, respectively. The USD versus flow discharge class relationships at each hydrometric station are plotted in Fig. 13. It can be seen that the flow discharge which owns the highest unsaturation degree (denoted by Q_u and listed in Table 2) is usually less than Q_e and increases with the distance from the dam. After calculating the difference between the pre-dam Q_e and Q_u (Table 2), an interesting finding is discovered, that is a piecewise linear relation with negative slopes exists between Q_e–Q_u and the longitudinal distance, and when the vertical axis is expressed by the relative difference, a complete exponential curve can fit all the points of Q_{e2} better (Fig. 14). These results mean that the most

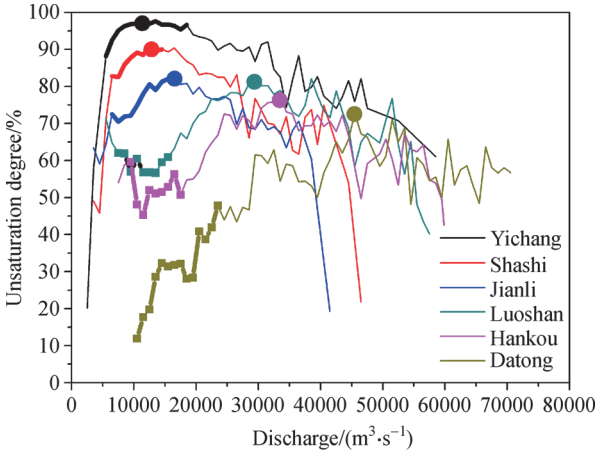

Fig. 13 The variation in the unsaturation degree of different flow discharges. The most unsaturated flow discharges (Q_u) are marked with solid dots and the flow discharge ranges with an increased occurrence frequency are in bold.

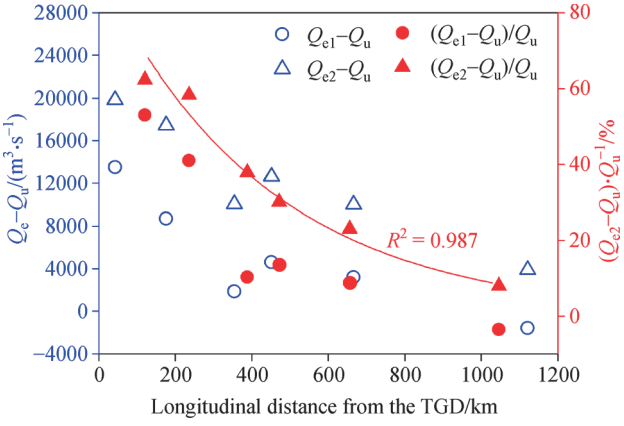

Fig. 14 Relationship between the clossness to dam and the absolute difference (Q_e–Q_u), and relative difference ((Q_e–Q_u)/Q_e).

unsaturated flow class after dam construction can be empirically determined according to the pre-dam effective discharges and distances from dam. Despite the limited samples query the universal use of this relation, there is no doubt that certain factors concerned with the longitudinal distance from dam such as catchment area, frictional head loss, sediment replenishment, bed armoring and average scouring depth can affect the locations of the most unsaturated flow class and further induce different changes in effective discharge.

5.2 Variability of effective discharge

The existence of a bimodal effective discharge curve has been reported in many previous studies (Phillips, 2002; Crowder and Knapp, 2005; Lenzi et al., 2006; Ma et al., 2010). Both the frequent moderate flows and the less frequent extreme flows are likely to be the effective discharges due to their significant geomorphic works. The former is mainly responsible for morphological adjustments within the main channel and usually less than the bankfull discharge, while the latter can transport the coarser sediment and even result in destructive channel reworking. In the present work, two effective discharges are determined according to their relatively higher amounts of sediment transport and both of them are within the medium discharge range, with an occurrence frequency of several days per year.

It is found that the effective discharges are closely related to the mean annual run off volumes (Fig. 15). However, only the pre-dam effective discharges have the good exponential relationships with flow conditions, which mainly due to the quasi equilibrium state of pre-dam channels (Xu, 1996; Bolla Pittaluga et al., 2003; Zhang et al., 2016). This result might imply that the post-dam channel morphological processes tend to accommodate the effective discharges to the regulated flow conditions until a new state of equilibrium is reached. Besides the above regularity of the pre-dam effective discharges, the limited regional discrepancies in occurrence frequency (Q_{e1} values 1.48%–1.77% (5–7 days/a), and Q_{e2} values 0.71%–0.93% (2–4 days/a)) and exceedance probability (Q_{e1} values 13.88%–19.45% (51–71 days/a), and Q_{e2} values 5.28–10.43% (19–38 days/a)) of the pre-dam effective discharges within the whole watershed also hint a relatively steadier state of the pre-dam channels. The severe unidirectional channel adjustments and flow frequency irregularity caused by regulation regimes are considered to be the most two leading causes of the post-dam disorder of effective discharges (Esmaeili and Mahdavi, 2002).

In addition, results from this study show that a regional variability of effective discharge adjustments exists in the downstream reaches due to dam construction. In Jianli and its lower reaches, the effective discharges decrease, while

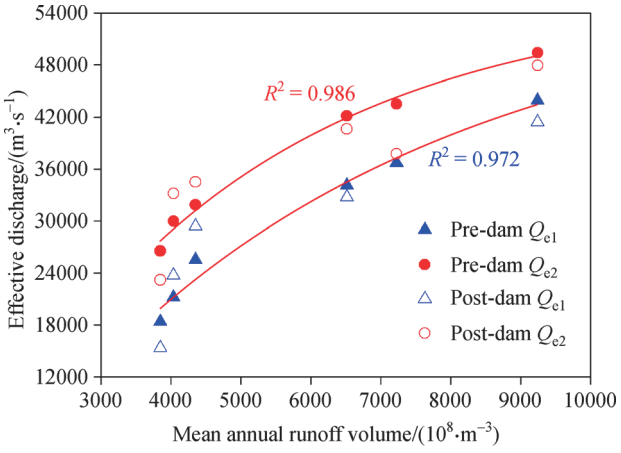

Fig. 15 Relationship between the mean annual runoff volume and effective discharge (Q_e).

in the more upstream reaches, the effective discharges increase. This phenomenon can be mainly attributed to the difference between the most unsaturated flow discharge Q_u and effective discharges Q_e, and is found to be related to the longitudinal distance from the dam (Fig. 14). To explain this connection, we investigate the sediment runoffs associated with different particle sizes and calculate their percentage reduction after dam construction, which can be written as:

$$PR = (SL_{pre} - SL_{post}) \times 100 / SL_{pre} \quad (3)$$

where PR means the percentage reduction, %; SL_{pre} and SL_{post} are the pre-dam and post-dam sediment load, respectively.

Figure16 demonstrates that the percentage reduction of sediment load, especially for the parts of $d < 0.125$ mm exhibits a good linear relationship with the longitudinal distance, which reflects the downstream variations in sediment transport capacity that the closer to the dam, the higher percentage reduction of sediment load and the larger difference between the pre-dam Q_e and Q_u (Fig. 14 and Table 2). The reason lies in that even when approaching the minimum flow discharge, the post-dam flows have already been under a high saturation state (Fig. 13) due to sediment retaining by dam, and with the increase of flow discharge, sediment replenishment is restrained by the riverbed coarsening, causing an increasing unsaturation degree until the flow velocity exceeded the incipient velocity of the coarser particles, after which the unsaturation degree diminishes gradually owing to the added sediment supply from the riverbed. It is evident that the magnitude of Q_u is closely correlated with the replenishment process of the finer sediment. The reaches that are closer to dam usually experience a relatively faster replenishment process and have a higher degree of bed coarsening (Guo et al., 2020), which can finally lead to a larger reduction of Q_u relative to

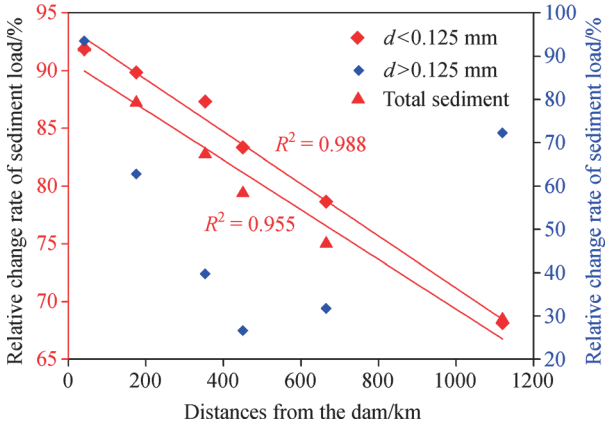

Fig. 16 Relationship between closeness to dam and relative change percentage of sediment load after damming.

Q_e. Since the discharges around Q_u are all in a high level of unsaturation (Fig. 13), the further the pre-dam Q_e exceeds Q_u, the lower unsaturation degrees the larger floods have, which is exactly the case at Yichang and Shashi.

Actually, for different sediment particle sizes, the most effective discharges (mean the flow discharges that carry the most amounts of sediment of certain particle sizes) are different (Chen et al., 2018). The longitudinal difference in particle composition is not only the result but also the controlling factor of different replenishment processes (Yang et al., 2017a). Thus, since the effective discharge in this paper is calculated in terms of the whole suspended sediment particle size range, it can be regarded as having considered the effect of particle composition of the sediment-laden flows. And the good correlation between longitudinal distance and sediment percentage reduction is exactly a reflection of the influences by particle composition on effective discharge.

Therefore, although the dam operation increases the occurrence frequency of low and medium flows, the flows that become more frequent are all located within the extremely high-unsaturation-discharge ranges at Yichang and Shashi (Fig. 13), whereby the less frequent and less unsaturated large discharges can transport a greater portion of sediment, resulting in the increase of effective discharges. Whereas in Jianli and its lower reaches, the shorter distances to Q_u of the flows that become more frequent provide higher unsaturation degrees of the pre-dam Q_e, thus the more frequent low and medium flows can transport more sediment, causing the decrease in effective discharges.

In summary, at the reaches close to dam, relatively higher unsaturation degree of the pre-dam effective discharges is the main cause of the increase in effective discharges, while at the further downstream reaches, the increase in occurrence frequency of low and medium flows is the primary factor driving the decrease in effective discharges. This confirms Andrew's view that both the less proportion of large flows and lower threshold of sediment movement can contribute to a decrease in effective discharge (Andrews, 1979).

5.3 Variability of bankfull discharge

Changes in river morphology caused by different flow-sediment regimes are reported to have great impacts on the discharge-stage relationship and conveyance capacity of river channels (Staines and Carrivick, 2015; Guan et al., 2016). Intuitively, according with the channel degradation caused by clear water flushing downstream of the TGD, water stages corresponding to given discharges in fixed sites are expected to be lowered and the discharges required to fill the channel to the level of floodplains can be much larger. However, as discussed earlier, the post-dam flood water stages are found to be lifted higher and considering the effects of the slightly decreasing bankfull levels, it is not surprising to observe a decrease in the bankfull discharges after dam construction.

As with effective discharge adjustments, the bankfull discharge adjustments after damming also exhibit a regional difference, which mainly originates from different changing manners of flood level as well as bankfull level. The rising flood levels and descending bankfull levels contribute to the decreased bankfull discharges from Yichang to Jianli, while the slightly degraded river channels and slightly descending flood levels result in the increase of bankfull discharges from Luoshan to Datong. This otherness of bankfull discharge adjustments may raise a new problem that the magnitude difference between the upstream and downstream bankfull discharges are enlarged, which means the flood capacity between Yichang and Jianli is further lower than that between Luoshan and Datong.

Before damming, the exceedance probability of bankfull discharges in the lower reaches (4.22%–8.75% (15–32 days/a) from Luoshan to Datong) is much more than that in the upper reaches (1.58%–1.90% (5–7 days/a) from Yichang to Jianli), while after damming, significant reductions in the exceedance probability occur in the lower reaches (0.95%–2.82% (3–10 days/a)) because of the increased bankfull discharges and reduced flood peaks. Thanks to flow regulations, the occurrence frequency of the overbank discharges is controlled not to change much, preventing the increasing risk of flood hazards.

The roughly equivalence between the bankfull discharge and 1.5-year recurrence interval discharge based on the annual flood peak series has been suggested by numerous studies (Woloman and Miller, 1960; Leopold et al., 1964; Andrews, 1979; Lenzi et al., 2006; Ma et al., 2010). In this paper, the 1.5-year and 2-year recurrence interval discharges (denoted by $Q_{1.5}$ and $Q_{2.0}$, respectively) at each hydrometric station are calculated. And again, $Q_{1.5}$ is proved to be a good proxy of bankfull discharge (Fig. 17 and Table 2) and $Q_{2.0}$ is overall larger than Q_b whether in terms of the pre-dam or post- dam period,

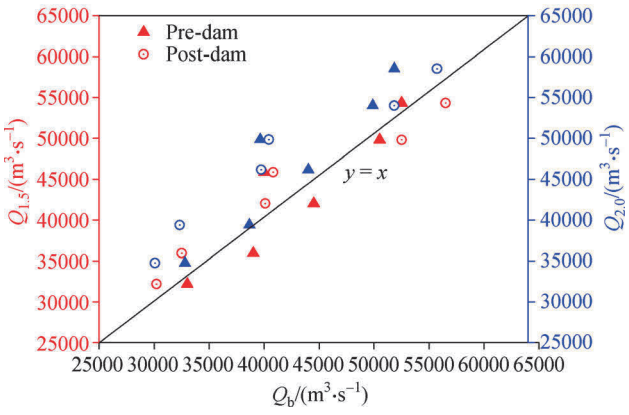

Fig. 17 Relationships between bankfull discharge (Q_b) and the 1.5- year ($Q_{1.5}$) and 2.0-year ($Q_{2.0}$) recurrence interval discharges.

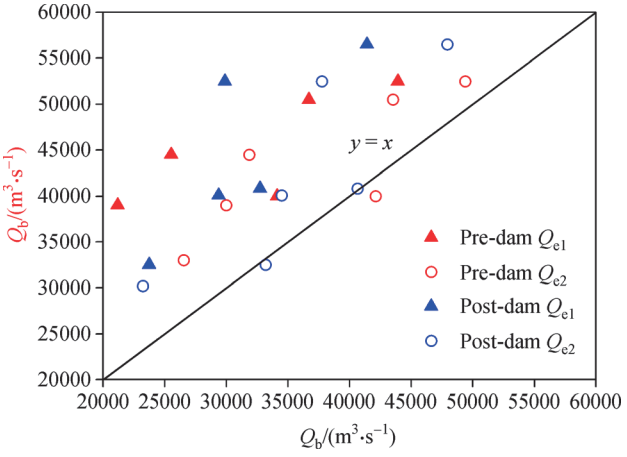

Fig. 18 Relationships between effective discharge (Q_e) and bankfull discharge (Q_b).

which indicates that $Q_{2.0}$ is usually an overestimation of the bankfull discharge in the Middle and Lower Yangtze River.

5.4 Relationships among effective, bankfull and channel-forming discharges

Comparison of the bankfull discharge with effective discharge has been conducted by many previous studies (Lenzi et al., 2006; Roy and Sinha, 2014). The close agreement between them is mostly found to exist in the plain rivers with constructed floodplains, especially in the rivers under an equilibrium condition (Woloman and Miller, 1960; Andrews, 1979; Sichingabula, 1999). However, several studies also reported the significant differences between Q_b and Q_e, which can be resulted from the larger threshold of sediment motion in gravel-bed rivers (Gomez et al., 2007), the different sediment yield characteristics in acid rivers (Ma et al., 2010) and the diversity of sediment fraction considered in effective discharge computation (Nash, 1994). Our results further corroborate that the effective discharge in the Middle and Lower Yangtze River are well below bankfull discharge, whether during the pre-dam or post-dam period (Fig. 18). This indicates that even in the large gravel-bed and sand-bed rivers with an approximate equilibrium state of channel scouring and silting, the effective discharge can also be unequal to bankfull discharge due to other reasons. Moreover, there is no directional adjustments in the difference between Q_b and Q_e after damming, which could be due to their different leading factors. The effective discharge in a quasi-steady river is closely related to the mean annual runoff volume (Fig. 15), whereas the bankfull discharge is directly determined by river landscapes and discharge-stage relations.

Application of the concept "channel-forming discharge" has been always confusing due to different discussing objects of channel category. Many researches supported the assertion that effective discharge is the channel-forming discharge since they referred the channel as the whole passage through which water flows, and agree on the equivalence of Q_e and Q_b (Crowder and Knapp, 2005; Lenzi et al., 2006; Ma et al., 2010). From this perspective, we can also draw the conclusion that the effective discharges are not the determinant of channel morphology, as they could seldom overflow onto the floodplains (Roy and Sinha, 2014). Nevertheless, in terms of sediment transport ability, Q_{e2} is quite close to Q_b and the discharges below Q_{e2} can produce a large part of the whole channel deformation as shown in Fig. 19. In most cases the discharges below Q_{e2} can transport about 65% of the total sediment. Actually, if we refer the channel forming discharges as all those flow discharges that could induce remarkable changes of the representative morphological

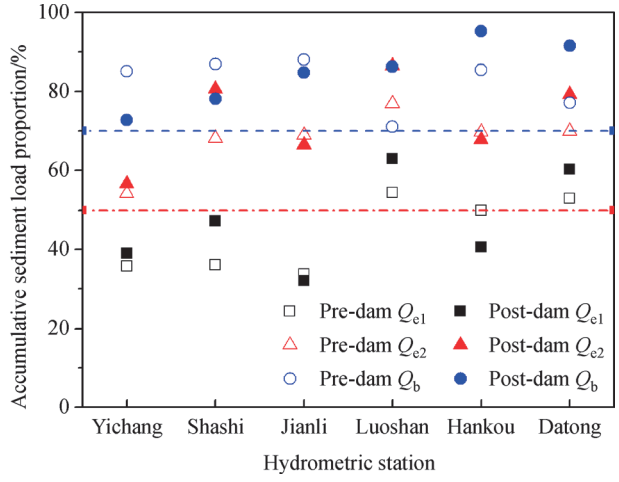

Fig. 19 Accumulative sediment load proportions of the effective discharges (Q_{e1} and Q_{e2}) and bankfull discharge (Q_b) at the hydrometric stations.

units rather than the whole main channel, the two calculated effective discharges Q_{e1} and Q_{e2} can be both considered as the "channel forming discharges" due to their relative effectiveness in sediment transport (Gomez et al., 2007; Surian et al., 2009). Considering the compound cross-section morphology and interweavement of single-thread and multithreaded reaches in the Middle and Lower Yangtze River, Q_{e1} and Q_{e2} are very likely to be the formative discharges for different morphological units within main channels.

6 Conclusions

We have estimated the effective and bankfull discharges in the reaches downstream of the TGD based on field data. The main conclusions can be summarized as follows:

1) Sediment load especially for the finer particles is significantly decreased since dam construction, which breaks the original channel equilibrium and ultimately leads to the variations in effective and bankfull discharges.

2) Two effective discharges at each hydrological station are determined. The pre-dam effective discharge is found to be closely related to the mean annual runoff volume, with a narrow-range regional difference in the occurrence frequency (Q_{e1} values 1.48%–1.77% (5–7 days/a), and Q_{e2} values 0.71%–0.93% (2–4 days/a)) and exceedance probability (Q_{e1} values 13.88%–19.45% (51–71 days/a), and Q_{e2} values 5.28%–10.43% (19–38 days/a)) due to a relatively steady state of river channels.

3) The variations in effective discharge after damming are the result of a contest between the changed flow frequency distribution and sediment transport ability. Relatively higher unsaturation degree of the pre-dam effective discharges caused by dam interception and riverbed coarsening is the main cause of the increase in effective discharges from Yichang to Shashi, while the increased occurrence frequency of the low and medium discharges by flow regulation is the primary factor driving the decrease in effective discharges from Jianli to Datong.

4) Bankfull discharge proves to be an approximate agent of the 1.5-year recurrence interval discharge. The rising flood levels and descending bankfull levels lead to a 2.0%–7.6% decrease in bankfull discharges from Yichang to Jianli, while the slightly lowered riverbed results in a 9.9%–16.5% increase in bankfull discharges from Luoshan to Datong. By reading the abrupt change point in the flow discharge versus class-based sediment transport rate plot, the bankfull discharge can be much accurately estimated.

5) In most cases, the effective discharge in the Middle and Lower Yangtze River is well below bankfull discharge even during the pre-dam period. Overall, the discharges below Q_{e2} can transport about 65% of the total sediment. Due to the relative effectiveness in sediment transport, Q_{e1} and Q_{e2} can be the channel forming discharges associated with the shaping of different morphological units within main channels.

Acknowledgements This work was supported by the National Key Research and Development Program of China (No. 2016YFC0402101) and the National Natural Science Foundation of China (Grant No.51779184). We would like to thank the Yangtze River Water Resources Commission for providing important field data. The instructive suggestions by the editors and anonymous reviewers are gratefully acknowledged.

References

Andrews E D (1979). Effective and bankfull discharges of streams in the Yampa River Basin, Colorado and Wyoming. J Hydrol (Amst)

Andrews E D, Nankervis J M (1995). Effective discharge and the design of channel maintenance flows for gravel-bed rivers. Natural & Anthropogenic Influences in Fluvial Geomorphology, 89: 151–164

Ashmore P E, Day T J (1988). Effective Discharge for Suspended Sediment Transport in Streams of the Saskatchewan River Basin. Water Resour Res, 24(6): 864–870

Ashraf M, Bhatti M T, Shakir A S (2016). River bank erosion and channel evolution in sand-bed braided reach of River Chenab: role of floods during different flow regimes. Arab J Geosci, 9(2): 140

Biedenharn D S, Copeland R R, Throne C R, Soar P J, Hey R D, Watson C C (2000). Effective Discharge Calculation: A Practical Guide, Vicksburg, MS, Techn. Rep. ERDC/CHL TR-00-15, 61

Bolla Pittaluga M, Repetto R, Tubino M (2003). Channel bifurcation in braided rivers: equilibrium configurations and stability. Water Resour Res, 39(3)

Bunte K, Abt S R, Swingle K W, Cenderelli D A (2014). Effective discharge in Rocky Mountain headwater streams. J Hydrol (Amst), 519: 2136–2147

Chai Y, Li Y, Yang Y, Li S, Zhang W, Ren J, Xiong H (2019a). Water level variation characteristics under the impacts of extreme drought and the operation of the Three Gorges Dam. Front Earth Sci, 13(3): 510–522

Chai Y, Li Y, Yang Y, Zhu B, Li S, Xu C, Liu C (2019b). Influence of climate variability and reservoir operation on streamflow in the Yangtze River. Sci Rep, 9(1): 5060

Chen D, Yu M H, Zhu Y H (2018). Study on effective discharge in the Lower Jingjiang River before and after construction of the Three Gorges Dam. Adv Water Sci, 29(6): 788–798 (in Chinese)

Chen F, Chen L, Zhang W, Han J, Wang J (2019). Responsed of channel morphology to flow-sediment variations after dam construction: a case study of the Shashi Reach, middle Yangtze River. Hydrol Res, 50(5): 1359–1375

Crowder D W, Knapp H V (2005). Effective discharge recurrence intervals of Illinois streams. Geomorphology, 64(3–4): 167–184

Dai Z, Du J, Li J, Li W, Chen J (2008). Runoff characteristics of the Changjiang River during 2006: effect of extreme drought and the impounding of the Three Gorges Dam. Geophys Res Lett, 35(7): L07406

Dai Z, Liu J T (2013). Impacts of large dams on downstream fluvial sedimentation: an example of the Three Gorges Dam (TGD) on the Changjiang (Yangtze River). J Hydrol (Amst), 480: 10–18

Dai Z, Fagherazzi S, Mei X, Gao J (2016). Decline in suspended sediment concentration delivered by the Changjiang (Yangtze) River into the East China Sea between 1956 and 2013. Geomorphology, 268: 123–132

Doyle M W, Stanley E H, Strayer D L, Jacobson R B, Schmidt J C (2005). Dominant discharge analysis of ecological processes in streams. Water Resour Res, 41: W11411

Dunne T, Leopold L B (1978). Water in Environment Planning. San Francisco: Freeman

Eaton B C, Lapointe M F (2001). Effects of large floods on sediment transport and reach morphology in the cobble-bed Sainte Marguerite River. Geomorphology, 40(3–4): 291–309

Emmett W W, Wolman M G (2001). Effective discharge and gravel-bed rivers. Earth Surf Process Landf, 26(13): 1369–1380

Esmaeili D, Mahdavi M (2002). The study of effective discharge for suspended sediment transport in streams of the Zayandeh-rood Dam Basin. Iran. J Nat Res, (55): 295–305

Gomez B, Coleman S E, Sy V W K, Peacock D H, Kent M (2007). Channel change, bankfull and effective discharges on a vertically accreting, meandering, gravel-bed river. Earth Surf Process Landf, 32 (5): 770–785

Graf W L (2006). Downstream hydrologic and geomorphic effects of large dams on American rivers. Geomorphology, 79(3–4): 336–360

Guan M, Carrivick J L, Wright N G, Sleigh P A, Staines K E H (2016). Quantifying the combined effects of multiple extreme floods on river channel geometry and on flood hazards. J Hydrol (Amst), 53(8): 256–268

Gunsolus E H, Binns A D (2018). Effect of morphologic and hydraulic factors on hysteresis of sediment transport rates in alluvial streams. River Res Appl, 34(2): 183–192

Guo X H, Qu G, Liu Y, Liu X Y (2020). Sediment transport of different particle size groups in the downstream channel after operation of the Three Gorges Project. J Lake Sci, 32(2): 564–572 (in Chinese)

Han J Q, Sun Z H, Yang Y P (2017). Flood and low stage adjustment in the Middle Yangtze River after impoundment of the Three Gorges Reservoir (TGR). J Lake Sci, 29(5): 1217–1226 (in Chinese)

Lenzi M A, Mao L, Comiti F (2004). Magnitude-frequency analysis of bed load data in an Alpine boulder bed stream. Water Resour Res, 40 (7):7201

Lenzi M A, Mao L, Comiti F (2006). Effective discharge for sediment transport in a mountain river: computational approaches and geomorphic effectiveness. J Hydrol (Amst), 326(1–4): 257–276

Leopold L B, Wolman M G, Millar J P (1964). Fluvial Processes in Geomorphology. San Fransisco: W H Freeman and Company

Li D, Lu X X, Yang X, Chen L, Lin L (2018a). Sediment load responses to climate variation and cascade reservoirs in the Yangtze River: a case study of the Jinsha River. Geomorphology, 32(2): 41–52

Li S, Li Y T, Yuan J, Zhang W, Chai Y F, Ren J Q (2018b). The impacts of the Three Gorges Dam upon dynamic adjustment mode alterations in the Jingjiang reach of the Yangtze River, China. Geomorphology, 31(8): 230–239

Li Y, Sun Z, Liu Y, Deng J (2009). Channel degradation downstream from the Three Gorges project and its impacts on flood level. J Hydraul Eng, 135(9): 718–728

Liu J, Deng J, Chai Y, Yang Y, Zhu B, Li S (2019). Variation of the water level in the Yangtze river in response to natural and anthropogenic changes. Water, 11(12): 2594

Ma Y, Huang H Q, Xu J, Brierley G J, Yao Z (2010). Variability of effective discharge for suspended sediment transport in a large semi-arid river basin. J Hydrol (Amst), 388(3–4): 357–369

Mckee L J (2002). Magnitude-frequency analysis of suspended sediment loads in the subtropical Richmond River basin, northern New South Wales, Australia. In: Proceedings of an international symposium held at Alice Springs

Mei X, Dai Z, Darby S E, Gao S, Wang J, Jiang W (2018). Modulation of extreme flood levels by impoundment significantly offset by floodplain loss downstream of the Three Gorges Dam. Geophys Res Lett, 45(7): 3147–3155

Nash D B (1994). Effective sediment-transporting discharge from magnitude-frequency analysis. J Geol, 102(1): 79–95

Pal S (2016). Impact of Massanjore Dam on hydro-geomorphological modification of Mayurakshi River, Eastern India. Environ Dev Sustain, 18(3): 921–944

Phillips J D (2002). Geomorphic impacts of flash flooding in a forested headwater basin. J Hydrol (Amst), 269(3–4): 236–250

Qin Z W, Chen X (2018). Study on downstream water level change of Three Gorges Reservoir impounding in dry season. Yangtze River, 49 (23): 10–15 (in Chinese)

Rickenmann D, Badoux A, Hunzinger L (2016). Significance of sediment transport processes during piedmont floods: the 2005 flood events in Switzerland. Earth Surf Process Landf, 41(2): 224–230

Roy N G, Sinha R (2014). Effective discharge for suspended sediment transport of the Ganga River and its geomorphic implication. Geomorphology, 227: 18–30

Schmidt K, Morche D (2006). Sediment output and effective discharge in two small high mountain catchments in the Bavarian Alps, Germany. Geomorphology, 129(8): 131–145

Shields J F D Jr, Copeland R R, Klingeman P C, Doyle M W, Simon A (2003). Design for stream restoration. J Hydraul Eng, 8(129): 575–584

Sichingabula H M (1999). Magnitude-frequency characteristics of effective discharge for suspended sediment transport, Fraser River, British Columbia, Canada. Hydrol Processes, 13(9): 1361–1380

Singh B, Rajpurohit D, Vasishth A, Singh J (2012). Probability analysis for estimation of annual one day maximum rainfall of Jhalarapatan Area of Rajasthan. Plant Arch, 12(2): 1093–1100

Staines K E H, Carrivick J L (2015). Geomorphological impact and morphodynamic effects on flow conveyance of the 1999 jökulhlaup at sólheimajökull, Iceland. Earth Surf Process Landf, 40(10): 1401–1416

StatSoft (2002). STATISTICA, version 6, Tulsa, Okla

Surian N, Mao L, Giacomin M, Ziliani L (2009). Morphological effects of different channel-forming discharges in a gravel-bed river. Earth Surf Process Landf, 34(8): 1093–1107

Vogel R M, Stedinger J R, Hooper R P (2003). Discharge indices for water quality loads. Water Resour Res, 39(10)

Walling D E (1977). Assessing the accuracy of suspended sediment rating curves for a small basin. Water Resour Res, 13(3): 531–538

Wang J, Sheng Y, Gleason C J, Wada Y (2013). Downstream Yangtze River levels impacted by Three Gorges Dam. Environ Res Lett, 8(4): 4012

Willams G P (1978). Bank-full discharge of rivers. Water Resour Res, 14 (6): 1141–1154

Wolman M G, Miller J P (1960). Magnitude and frequency of forces in

geomorphic processes. J Geol, 68(1): 54–74

Xu J (1996). Wandering braided river channel pattern developed under quasi-equilibrium: an example from the Hanjiang River, China. J Hydrol (Amst), 181(1–): 85–103

Yang S L, Zhang J, Xu X J (2007). Influence of the Three Gorges Dam on downstream delivery of sediment and its environmental implications, Yangtze River. Geophys Res Lett, 34(10): L10401

Yang Y P, Zhang M J, Li S Z, Zhu L L, You X Y, Li K Y, Yu X M (2017a). Transport patterns of the coarse and fine sediment and its causes in the downstream of the Three Gorges Dam. J Lake Sci, 29(4): 942–954 (in Chinese)

Yang Y P, Zhang M J, Sun Z H, Han J Q, Li H G, You X Y (2017b). The relationship between water level change and river channel geometry adjustment in the downstream of the Three Gorges Dam (TGD). Acta Geographica Sinica, 72(5): 776–789 (in Chinese)

Yevjevich V (1972). Probability and Statistics in Hydrology, Fort Collins: Water Resources Publications

Yuan W, Yin D, Finlayson B, Chen Z (2012). Assessing the potential for change in the middle Yangtze River channel following impoundment of the Three Gorges Dam. Geomorphology, 147–148: 27–34

Zahar Y, Ghorbel A, Albergel J (2008). Impacts of large dams on downstream flow conditions of rivers: aggradation and reduction of the Medjerda channel capacity downstream of the Sidi Salem dam (Tunisia). J Hydrol (Amst), 351(3–4): 318–330

Zhang W, Yuan J, Han J, Huang C, Li M (2016). Impact of the Three Gorges Dam on sediment deposition and erosion in the middle Yangtze River: a case study of the Shashi Reach. Hydrol Res, 47(S1): 175–186